Microalgae and Bacteria Interaction—Evidence for Division of Diligence in the Alga Microbiota

Yekaterina Astafyeva,[a] Marno Gurschke,[a] Minyue Qi,[b] Lutgardis Bergmann,[a] Daniela Indenbirken,[c] Imke de Grahl,[d] Elena Katzowitsch,[e] Sigrun Reumann,[d] Dieter Hanelt,[f] Malik Alawi,[b] Wolfgang R. Streit,[a] Ines Krohn[a]

[a]University of Hamburg, Institute of Plant Science and Microbiology, Department of Microbiology and Biotechnology, Hamburg, Germany
[b]University Medical Center Hamburg-Eppendorf, Bioinformatics Core, Hamburg, Germany
[c]Heinrich-Pette-Institute, Leibniz Institute for Experimental Virology, Virus Genomics, Hamburg, Germany
[d]University of Hamburg, Institute of Plant Science and Microbiology, Department of Plant Biochemistry and Infection Biology, Hamburg, Germany
[e]University of Würzburg, Core Unit Systems Medicine, Würzburg, Germany
[f]University of Hamburg, Institute of Plant Science and Microbiology, Department of Aquatic Ecophysiology and Phycology, Hamburg, Germany

ABSTRACT Microalgae are one of the most dominant forms of life on earth that is tightly associated with a distinct and specialized microbiota. We have previously shown that the microbiota of *Scenedesmus quadricauda* harbors less than 10 distinct microbial species. Here, we provide evidence that dominant species are affiliated with the genera of *Variovorax*, *Porphyrobacter*, and *Dyadobacter*. Experimental and transcriptome-based evidence implies that within this multispecies interaction, *Dyadobacter* is a key to alga growth and fitness and is highly adapted to live in the phycosphere. While presumably under light conditions the alga provides the energy source to the bacteria, *Dyadobacter* produces and releases mainly a large variety of polysaccharides modifying enzymes. This is coherent with high-level expression of the T9SS in alga cocultures. The transcriptome data further imply that quorum-quenching proteins (QQ) and biosynthesis of vitamins B_1, B_2, B_5, B_6, and B_9 are expressed by *Dyadobacter* at high levels in comparison to *Variovorax* and *Porphyrobacter*. Notably, *Dyadobacter* produces a significant number of leucine-rich repeat (LRR) proteins and enzymes involved in bacterial reactive oxygen species (ROS) tolerance. Complementary to this, *Variovorax* expresses the genes of the biosynthesis of vitamins B_2, B_5, B_6, B_7, B_9, and B_{12}, and *Porphyrobacter* is specialized in the production of vitamins B_2 and B_6. Thus, the shared currency between partners are vitamins, microalgae growth-promoting substances, and dissolved carbon. This work significantly enlarges our knowledge on alga-bacteria interaction and demonstrates physiological investigations of microalgae and associated bacteria, using microscopy observations, photosynthetic activity measurements, and flow cytometry.

IMPORTANCE The current study gives a detailed insight into mutualistic collaboration of microalgae and bacteria, including the involvement of competitive interplay between bacteria. We provide experimental evidence that Gram-negative bacteria belonging to the *Dyadobacter*, *Porphyrobacter*, and *Variovorax* are the key players in a *Scenedesmus quadricauda* alga-bacteria interaction. We impart strong evidence that *Dyadobacter* produces and releases polysaccharides degradation enzymes and leucine-rich repeat proteins; *Variovorax* supplies the consortium with auxins and vitamin B_{12}, while *Porphyrobacter* produces a broad spectrum of B vitamins. We show not only that the microalgae collaborate with the bacteria and vice versa but also that the bacteria interact with each other via quorum-sensing and secretion system mechanisms. The shared currency between partners appears to be vitamins, microalgae growth-promoting substances, and dissolved carbon.

KEYWORDS microalgae and microbiota interaction, synthetic plant-bacteria system, phycosphere biofilm, *Scenedesmus quadricauda*, *Dyadobacter* sp.

The term microalgae is a collective phylogenetical expression for a highly heterogeneous group of eukaryotic and prokaryotic microorganisms that are unicellular photosynthetic organisms growing in marine and aquatic environments, respectively (1, 2). In general, microalgal cells are surrounded by a phycosphere, which is a region rich in organic material released by the algae creating the key interface in which algae and other organisms tightly interact (3). Thus, algae and bacteria synergistically affecting each other's physiology and metabolism together have an impact on the ecosystems and represent all modes of interactions between various organisms, ranging from mutualism to parasitism (4, 5).

Tight associations of microalgae and bacteria have resulted in the evolution of a complex network of these cross-kingdom interactions and a potential specialization of various organisms. Orchestrated nutrient exchange, mutual support of growth factors, and quorum-sensing mediation define a wide spectrum of associations at highly complex assemblages of unicellular microalgae and associated bacteria (3). The positive effects of algae-bacteria interaction on algal growth and flocculation processes has changed the scenario of considering bacteria as mere contamination of algae cultures (6). Several studies have verified that the microbiome of microalgae consists mainly of species of the phyla Bacteroidota, Flavobacteria, Alphaproteobacteriota, Betaproteobacteriota, and Gammaproteobacteriota (2, 7). Many noncultivatable organisms can be detected as well, but the overall abundance of microorganisms is often limited to approximately 30 species (2, 8). It is still unclear whether all of these bacteria are important for algal health and survival of the community. Interestingly, limited potential invasive or pathogenic species have been also detected during the screening but somehow appear to live in a balanced manner in the community, which can be explained by a selection pressure that favors the microalgae-bacteria consortia (9–12).

However, for applications in aquaculture, the potential of the interactions between microalgae and microorganisms may improve algal biomass production and may enrich the biomass with compounds of biotechnological interest such as lipids, carbohydrates, and pigments. Consequently, growth and photosynthetic activity of bacteria profit from the interaction with microalgae, especially by adhesion, clumping factor, motility, chemotaxis, secretion systems, quorum-sensing (QS), and quorum-quenching (QQ) systems and synthesis of growth promoters (5, 13–15). Intra- and interspecies communication among microbes occurs via a complex set of signal molecules secreted during both beneficial and harmful interactions that coordinate and control the behavior of microorganisms in mixed communities. Production and release of signal molecules will be recognized by other members of the microbial community, will initiate the communication causing up- or downregulation of gene expression, and will alter the activity and physiology of the recipient (8, 16, 17). Bacterial communication provides the regulation of virulence-associated factors, propagation, population density, and change in metabolic rate, various bacterial functions, including biofilm formation, motility, adhesion, and coordination between microbial communities (18).

The goal of the study was detailed insight into mutualistic collaboration of microalgae and bacteria, including the involvement of competitive interplay between bacteria. Since not much is known about the individual role of the individual members of the multispecies consortia, we set out to determine the role of one of the bacterial isolates from nonaxenic algal culture, *Dyadobacter* sp. HH091, in the interplay with the other dominant bacterial species and the alga. For this purpose, we isolated the bacterium from the microbiome, made it genetically accessible, and studied its impact using physiological and omics-based methods.

RESULTS

Previous studies have shown that microalgae obtained from strain collections are associated with various bacterial communities with a rather low diversity (2, 8). In this research, we concentrated on the microalga *Scenedesmus quadricauda* and its bacterial community. In this community, we observed bacteria affiliated with the genera *Dyadobacter* (phylum

Bacteroidota) and *Variovorax* and *Porphyrobacter* (phylum Proteobacteriota) as the dominant species (2, 9, 19). To gain insight into the physiological role of the microbiota, we set out to isolate individual strains and used them in cocultivation studies. Using classical enrichment strategies, we were able to cultivate a single *Dyadobacter* affiliated with a *S. quadricauda* laboratory nonaxenic culture on tryptone yeast extract salts (TYES) medium as described in the Materials and Methods section. The isolation of *Porphyrobacter* and *Variovorax* from the same *S. quadricauda* laboratory nonaxenic culture was unsuccessful.

The obtained *Dyadobacter* isolate was designated *Dyadobacter* sp. HH091 (from here on called "HH091"). Its phylogenetic affiliation with the genus *Dyadobacter* (phylum Bacteriodota) was initially verified by using 16S rRNA gene amplification and DNA sequencing. Following this, the organism's chromosomal DNA was extracted and sent out to establish its genome sequence. The HH091 genome draft consisted of 30 contigs and has a size of 7,837,776 bp with a G+C content of 43.87% (Table S1; Fig. S1). Annotation identified 6,628 genes, 6,565 of which are protein coding (Table S1). The HH091 genome was deposited at Integrated Microbial Genomes & Microbiomes (IMG/M) (https://img.jgi.doe.gov) under accession IMG ID 2842103827.

Dyadobacter is well adapted for life in multispecies communities and in the vicinity of microalga, which is confirmed by the metatranscriptomic activity of genes affiliated with competitive and plant-bacteria interaction. Its genome codes for several fascinating genetic features, such as multiple QS and QQ loci, which play important roles in cell signaling, and surviving in competitive conditions. Notably, we observed 23 possible QQ genes and 41 *luxR* solos. Further, it codes for complete secretion systems of type 4 (T4SS), 5 (T5SS), 6 (T6SS), and 9 (T9SS). In addition, a remarkable wealth of glycosyl hydrolases (GHs) was observed. A total of 69 GHs, 47 polysaccharide lyases (PLs) and 50 carbohydrate esterases (CEs) were predicted. Table 1 and Tables S1 to S5 give an overview of the genomic features of HH091.

Dynamics of the bacterial colonization of the microalgae studied by confocal microscopy. Based on the above-made observations, we were interested to analyze the effects of HH091 on the microalga in cocultures (Fig. 1). We were able to electroporate and stably maintain the plasmid pBBR1MCS-5-eGFP in HH091. This plasmid carries an enhanced green fluorescent protein (eGFP) under the control of the lac promoter and allowed the detection of HH091 on the surface and inside the algal cells using confocal laser scanning microscope (CLSM). In our experiments, we could not observe any growth inhibition of *Dyadobacter* sp. HH091 (wild type [WT]) and the plasmid-expressing bacteria. Additional high-resolution CLSM images of *S. quadricauda* incubated with HH091 implied that the bacterium was often tightly associated with the algal cells (Fig. 1). Fig. 1C presents the middle layer of a Z-Steck image of *S. quadricauda* with HH091, in which the bacteria is found inside the algal cells. We examined cocultures of HH091 grown together with *S. quadricauda* and compared its photosynthetic activity and relative fitness with the antibiotic-treated algal control cultures over a time period of 13 days (Fig. 2A). To identify the difference in the growth of algal cultures (with and without HH091), we used the optical density measurement (Fig. 2A). In these tests, the first hints of visible difference were observed after 2 to 3 days. The photosynthetic activity measurements by pulse-amplitude-modulation (PAM) fluorometry demonstrated that the coculturing of *S. quadricauda* with HH091 resulted in 1.5-fold increase of the optimal quantum yield of Photosystem II (PS II) in comparison to control antibiotic-treated microalgae (Fig. 2A). Additional microscopic and fluorescence-activated cell sorting (FACS) analyses verified that the number of viable and photosynthetic active cells in the presence of HH091 was much higher in comparison to antibiotic-treated cultures (Fig. 2B and C). In these tests, the algae culture (with and without HH091) were analyzed for 13 days after inoculation and by monitoring the chlorophyll autofluorescence of the algal population or the low-level autofluorescence of the bacteria in the FL2 channel (Fig. 2B). In a FSC X FL2 density blot diagram, three specific populations were detectable. These populations could be assigned as follows: population I, bacteria; population II, dead and lysed algal cells; and; population III, healthy microalgae (Fig. 2B; Fig. S2). In the beginning of the experiment, the content of living algal

Table 1 Possible interaction pathways of *Dyadobacter* sp. HH091 genome[a]

Selected key features	*Dyadobacter* sp. HH091
Transporter, efflux pumps, and secretion systems	
Transport proteins and efflux pumps	138
MFS, ABC, and biopolymer transporters	189
T4SS	3
T5SS	9
T6SS	9
T9SS	41
Sec-independent protein secretion pathway	2
Sec-SRP	5
Signal transduction and regulation mechanisms	
Response regulators (NarL/FixJ, LytR, OmpR)	116
ECF sigma factors	54
Polysaccharides degradation	
Auxiliary activities	16
Carbohydrate esterases	50
Glycoside hydrolases	69
Glycosyl transferases	69
Polysaccharide lyases	47
Carbohydrate-binding modules	21
Peptidases	139
Competitive interactions	
Potential antibiotic substances	16
Endonucleases and exonucleases	60
Permeases	157
Proteases	69
Heme synthesis	9
Quorum quenching	23
Bacteria-plant interaction pathways	
Vitamins biosynthesis	224
Invasion-associated proteins	2
LRR proteins	2
ROS tolerance	13

[a]The table shows the key features of possible competitive and plant-bacteria interaction pathways of the *Dyadobacter* sp. HH091 genome, using Integrated Microbial Genomes (IMG) function search. The data are shown as the total number of hits. Major facilitator superfamily (MFS), ATP-binding cassette (ABC)-transporters, type 4 secretion system (T4SS), type 5 secretion system (T5SS), type 6 secretion system (T6SS), type 9 secretion system (T9SS), secretion (Sec), secretion-signal recognition particle (Sec-SRP), extracytoplasmic function (ECF), leucine-rich repeat (LRR), reactive oxygen species (ROS).

cells in an antibiotic-treated culture was 59.4% ($\pm$0.5), whereas 5.56% ($\pm$0.6) of the population included bacteria with 13.2% ($\pm$0.8) of lysed algal cells. In the end of the experiment, we identified 70.8% ($\pm$1.6) of healthy microalgae, 18.8% ($\pm$0.5) of lysed algal cells, and 3.49% ($\pm$0.5) of bacteria in a coculture with *Dyadobacter*. In general, we
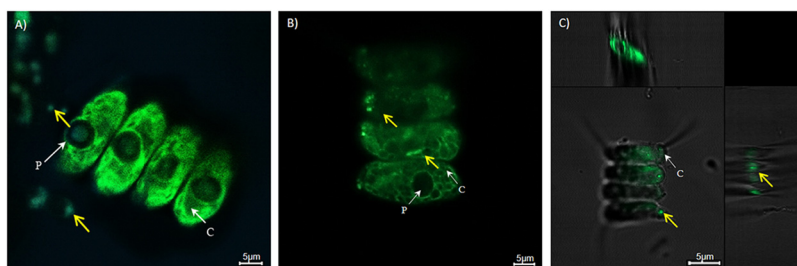

FIG 1 Confocal microscope images of the strain *Dyadobacter* sp. HH091 expressing enhanced green fluorescent protein (eGFP) (yellow arrows) in coculture with *S. quadricauda* MZCH 10104. A confocal laser scanning microscope (CLSM) Axio Observer.Z1/7 LSM 800 (Carl Zeiss Microscopy GmbH, Jena, Germany) with ZEN software (version 2.3; Carl Zeiss Microscopy GmbH) was used. (A) Three-day culture. (B) seven-day culture; (C) seven-day culture, Z-Steck image. An autofluorescence quenching kit was used to lower the autofluorescence of chlorophyll of the microalga. c = chloroplast; p = pyrenoid. Bar = 5 μm.
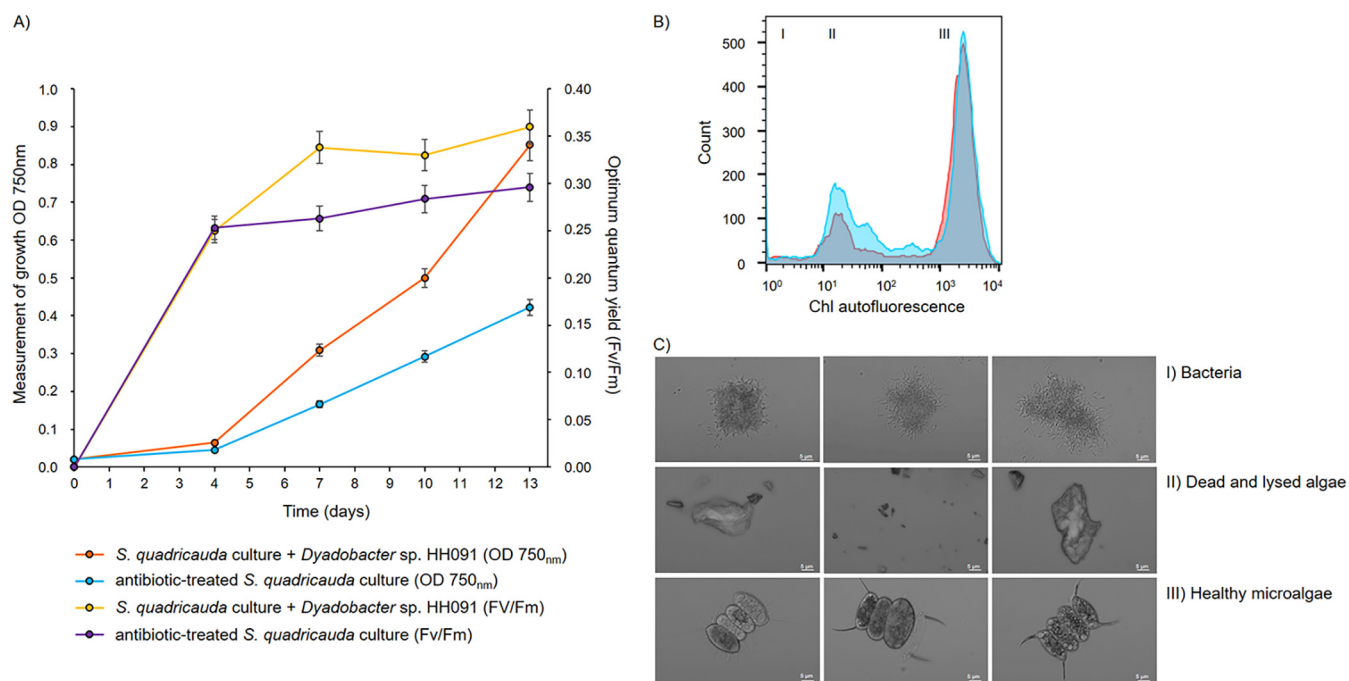
FIG 2 (A, B) Photosynthetic activity and growth measurement (A) and fluorescence-activated cell sorting (FACS) analyses (B) of *S. quadricauda* MZCH 10104 in coculture with the strain *Dyadobacter* sp. HH091. (A) Increased photosynthetic activity and growth rate (optical density at 750 nm [OD 750 nm]) can be observed in the coculture with HH091. (B) Comparison of populations, based on chlorophyll intensity. Orange shading indicates a stable distribution of bacteria (population I), dead and lysed algae (population II), and healthy microalgae (population III) in the coculture at the end of the experiment (13 days). Blue shading shows how the proportion of dead and lysed algae is increased in the culture without HH091. The raw data are available in Fig. S2. (C) Images of cell sorting acquired with CLSM Axio Observer.Z1/7 LSM 800 (Carl Zeiss Microscopy GmbH, Jena, Germany) and ZEN software (version 2.3; Carl Zeiss Microscopy GmbH). Bar = 5 μm. Pulse-amplitude-modulation (PAM) fluorometry and FACS analyses demonstrated the improved fitness of *S. quadricauda* cocultured with HH091.

count approximately 10 to 15 bacterial cells for 1 microalgal cell. Comparison of populations, based on chlorophyll intensity, indicates a stable distribution of bacteria (population I), dead and lysed algae (population II), and healthy microalgae (population III) in the coculture at the end of the experiment (13 days), whereas in the culture without HH091, the proportion of dead and lysed algae is increased (3.24% of bacteria [population I], 27.4% of lysed algal cells [population II], and 57.7% of algae cells [population III]) (Fig. 2B; Fig. S2).

Transcriptome sequencing (RNA-Seq) global analysis of multispecies bacterial consortia and microalga transcriptomes. We hypothesize that more than one compound is essential for a healthy algae growth, which is not known yet. To further analyze the role of HH091 in this specific cross-kingdom interaction, we set out to analyze the transcriptomes of this bacterium in the background of the native multispecies microbiota. We chose to use the original *S. quadricauda* lab culture, from which HH091 was isolated, as this would most likely resemble the native situation in a multispecies community. Thus, we analyzed the multispecies transcriptome of the microbiota at exponential and stationary growth phases of *S. quadricauda* cultures (Table S6; Fig. 3). Sequences obtained for this study were submitted to the European Nucleotide Archive (ENA; PRJEB23338).

In total, we obtained 42 million (mio) reads of bacteria data after trimming. The data are the results of three replicates with each replicate producing between 19 and 25 mio reads. The trimmed reads were assembled into contigs for the exponential and stationary phase experiments (Table S6). In total, the RNA-Seq data covered a significant portion of overall bacterial genomes and the affiliated pathways.

Fig. 3 summarizes the transcriptomics for the exponential (A) and the stationary (B) growth phases. In all treatments, the largest fraction of transcribed genes had no function assigned (20 to 25%). In the bacteria, the second largest fraction was associated
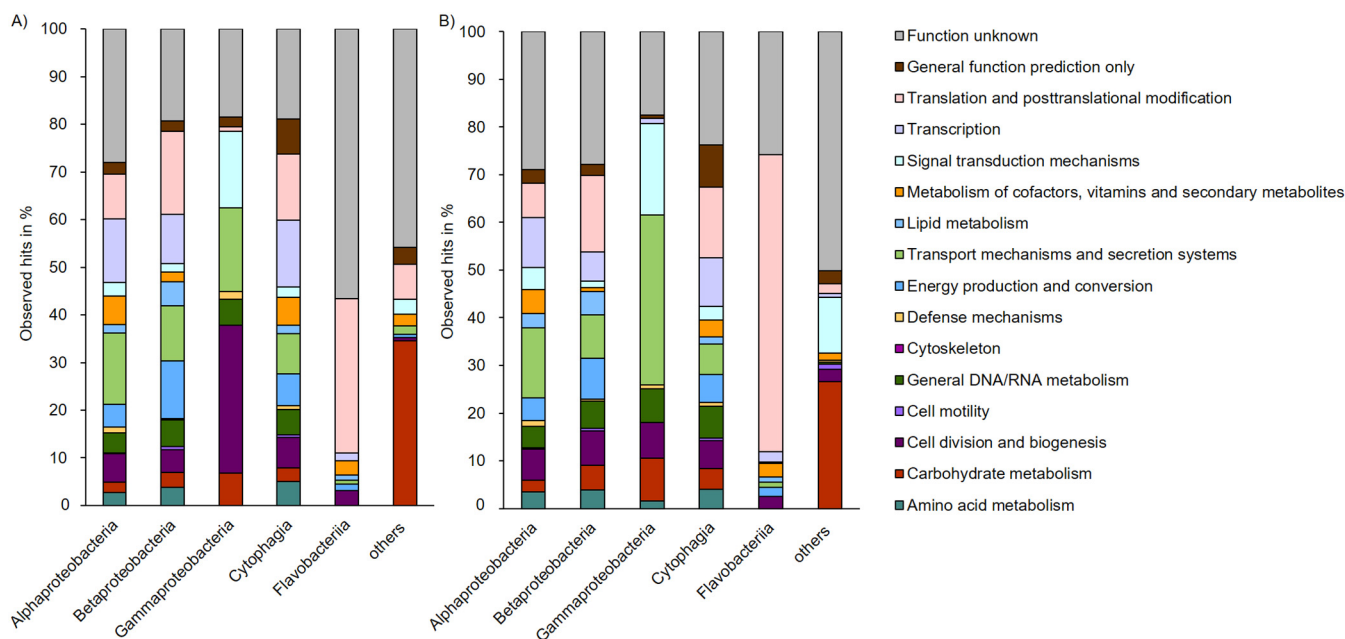
FIG 3 Expressed genes of bacteria in coculture with the microalga *S. quadricauda* during the exponential (A) and stationary (B) growth phases. The generated sequence data (approximal 42 mio reads) were mapped to the available genomes and metagenomes (8). The most dominant species of the microbiome are affiliated with the phyla of the Proteobacteriota (*Variovorax* and *Porphyrobacter*) and Bacteroidota (*Dyadobacter*).

with transport mechanisms and secretion systems during the exponential phase (15% Alphaproteobacteriota, 11.5% Betaproteobacteriota, 17.5% Gammaproteobacteriota, 8.5% Cytophagia, 0.73% Flavobacteriia, and 1.64% others). Further, a large fraction was connected to translation and posttranslational modification (9.5% Alphaproteobacteriota, 17% Betaproteobacteriota, 1% Gammaproteobacteriota, 14% Cytophagia, 32.5% Flavobacteriia, and 7.5% others). Notably, the bacteria showed relatively high levels of transcription of genes linked to the biosynthesis of cofactors, vitamins, and secondary metabolites (6% Alphaproteobacteriota, 2% Betaproteobacteriota, 6% Cytophagia, 3% Flavobacteriia, and 2.5% others).

The transcriptionally most active bacteria were *Dyadobacter* (3 mio reads mapped), *Porphyrobacter* (2.4 mio reads mapped), and *Variovorax* (1 mio reads mapped) at the exponential growth phase. This was similar at the stationary growth phase with *Dyadobacter* (6.9 mio reads), *Porphyrobacter* (5.5 mio reads), and *Variovorax* (1.3 mio reads). The data sets were normalized for the further analyses as outlined in the Materials and Methods section.

RNA-Seq identifies highest bacterial transcribed genes related to carbohydrate degradation, competitive, and plant-bacteria interaction. In the following, we highlight some of the most relevant findings of the whole data sets. Notably, we included those genes that had more than 500 counts/gene. The detailed analyses of the most strongly expressed genes are summarized in Fig. 4. The most strongly expressed genes affiliated with *Dyadobacter* were related to carbohydrate degradation, competitive, and plant-bacteria interaction. Genes, most strongly expressed in *Porphyrobacter* and *Variovorax*, included competitive interaction mechanisms, vitamins biosynthesis, secretion systems, and fatty acids biosynthesis (Fig. 4).

Nevertheless, the transcriptome data set hinted toward a metabolic symbiosis between microalgae/bacteria and bacteria/bacteria. Fig. 4 reflects the expression of genes affiliated with transporter and secretion systems, signal transduction and regulation mechanisms, polysaccharide degradation, competitive interactions, and interaction pathways of the microbiome of *S. quadricauda* during the exponential (A) and the stationary (B) growth phases.

Correlation between transcriptome and genome analyses exposes multifaceted synergistic cooperation. To examine the distribution of specific protein families across the transcriptionally most active bacterial genomes, we performed a protein
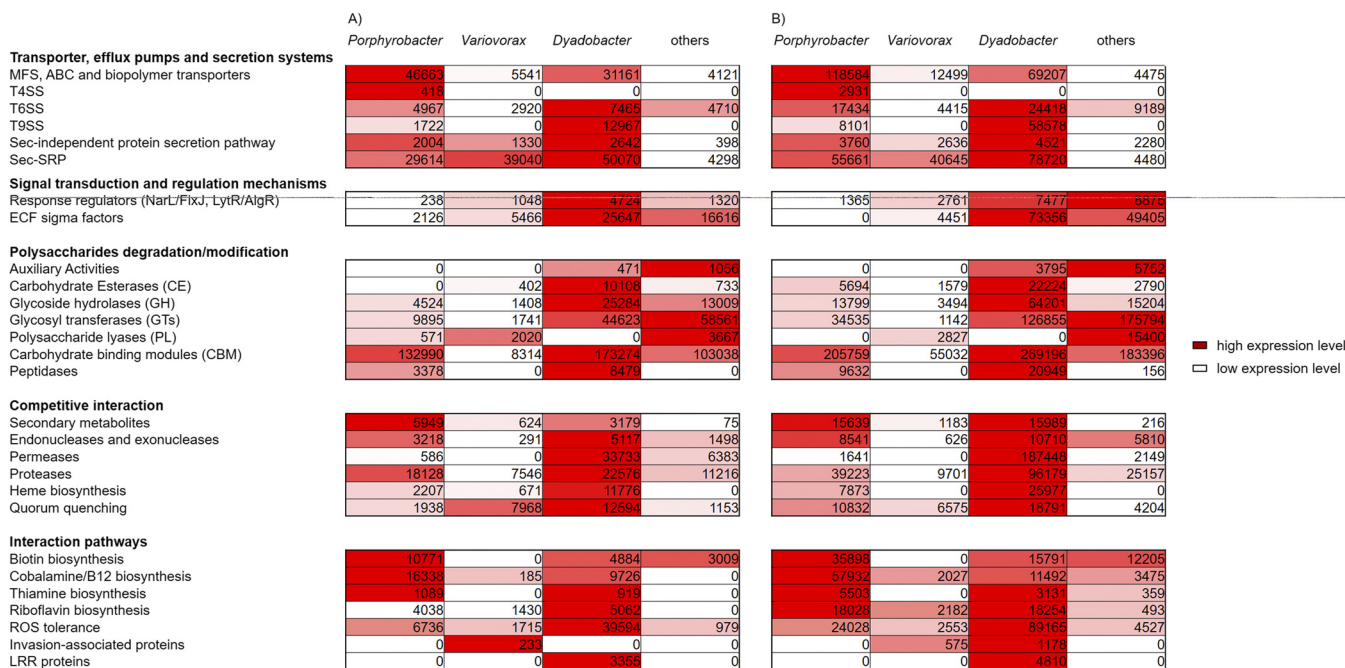
	A) Porphyrobacter	Variovorax	Dyadobacter	others	B) Porphyrobacter	Variovorax	Dyadobacter	others
Transporter, efflux pumps and secretion systems								
MFS, ABC and biopolymer transporters	46663	5541	31161	4121	118584	12499	69207	4475
T4SS	418	0	0	0	2931	0	0	0
T6SS	4967	2920	7465	4710	17434	4415	24418	9189
T9SS	1722	0	12967	0	8101	0	58578	0
Sec-independent protein secretion pathway	2004	1330	2642	398	3760	2636	4521	2280
Sec-SRP	29614	39040	50070	4298	55661	40645	78720	4480
Signal transduction and regulation mechanisms								
Response regulators (NarL/FixJ, LytR/AlgR)	238	1048	4724	1320	1365	2761	7477	6875
ECF sigma factors	2126	5466	25647	16616	0	4451	73356	49405
Polysaccharides degradation/modification								
Auxiliary Activities	0	0	471	1056	0	0	3795	5752
Carbohydrate Esterases (CE)	0	402	10108	733	5694	1579	22224	2790
Glycoside hydrolases (GH)	4524	1408	25284	13009	13799	3494	64201	15204
Glycosyl transferases (GTs)	9895	1741	44623	58561	34535	1142	126855	175794
Polysaccharide lyases (PL)	571	2020	0	3667	0	2827	0	15400
Carbohydrate binding modules (CBM)	132990	8314	173274	103038	205759	55032	269196	183396
Peptidases	3378	0	8479		9632	0	20949	156
Competitive interaction								
Secondary metabolites	6949	624	3179	75	15639	1183	15989	216
Endonucleases and exonucleases	3218	291	5117	1498	8541	626	10710	5810
Permeases	586	0	33733	6383	1641	0	187448	2149
Proteases	18128	7546	22576	11216	39223	9701	96179	25157
Heme biosynthesis	2207	671	11776	0	7873	0	25977	0
Quorum quenching	1938	7968	12594	1153	10832	6575	18791	4204
Interaction pathways								
Biotin biosynthesis	10771	0	4884	3009	35898	0	15791	12205
Cobalamine/B12 biosynthesis	16338	185	9726	0	57932	2027	11492	3475
Thiamine biosynthesis	1089	0	919	0	5503	0	3131	359
Riboflavin biosynthesis	4038	1430	5062	0	18028	2182	18254	493
ROS tolerance	6736	1715	39594	979	24028	2553	89165	4527
Invasion-associated proteins	0	233	0	0	0	575	1178	0
LRR proteins	0	0	3355	0	0	0	4816	0

high expression level / low expression level

FIG 4 Heat map reflecting the relative expression of genes affiliated with overall plant-bacteria interaction pathways of the bacterial metagenome of *S. quadricauda* during the exponential (A) and stationary (B) growth phases. Red shading indicates a high expression level, and white indicates a low expression level. The numbers indicate the total amount of hits during RNA-Seq. Genes have more than 500 counts/gene.

family comparison across the microbiome of *S. quadricauda* MZCH 10104 (Table S7). The protein families were filtered in affiliation with overall plant-bacteria interaction pathways.

Crucial key features of overall plant-bacteria interaction pathways highlighted in metatranscriptomic analysis were mapped to the reference genomes of *Porphyrobacter* sp. AAP82 (IMG 2551306481), *Variovorax paradoxus* S110 (IMG 644736413), and *Dyadobacter* sp. HH091 (IMG 222279) (Fig. 5). For *Porphyrobacter* and *Variovorax*, we used publicly available reference genome IMG 2551306481 (GenBank accession number ANFX00000000) and IMG 644736413 (GenBank accession numbers NC012791 and NC012792), respectively, and mapped the transcriptome data on these genomes. These two genomes were chosen as reference genomes because they have high-quality annotations and are originally isolated from aquatic/plant habitats (20, 21). The transcriptome data obtained for *Dyadobacter* were mapped onto the genome of HH091 (IMG 222279). The circular mapping was generated using the Circular Genome Viewer tool within PATRIC, the Pathosystems Resource Integration Center (www.patricbrc.org). Moving inward, the subsequent two rings show coding DNA sequences (CDSs) in forward (brown) and reverse (green) strands. Blue and yellow plots indicate GC content and a GC skew [(GC)/(G+C)]. Key features of possible competitive and plant-bacteria interaction pathways are marked with the following colors: purple for transporter, efflux pumps, and secretion systems; orange for signal transduction and regulation mechanisms; turquoise for polysaccharide degradation; red for competitive interactions; and blue for bacteria-plant interaction pathways (Fig. 5).

B vitamins are key drivers in bacteria-alga and bacteria-bacteria interactions. Thiamin biosynthesis genes were mainly expressed in *Dyadobacter* involving the whole cluster of required biosynthesis genes. *Dyadobacter* and *Porphyrobacter* are most likely auxotrophic for B_{12} biosynthesis (2). Biosynthesis of cobalamin requires approximately 30 enzymatic steps for its complete *de novo* construction. Among two existing distinct biosynthetic pathways, which are termed the aerobic and anaerobic routes (22), *Variovorax* codes in its genome for the anaerobic pathway of the vitamin B_{12} biosynthesis. Thus, it is likely that vitamin B_{12} was provided by *Variovorax* and not by any of the two other bacteria, as they lack these genes. A riboflavin (B_2) biosynthesis cluster is
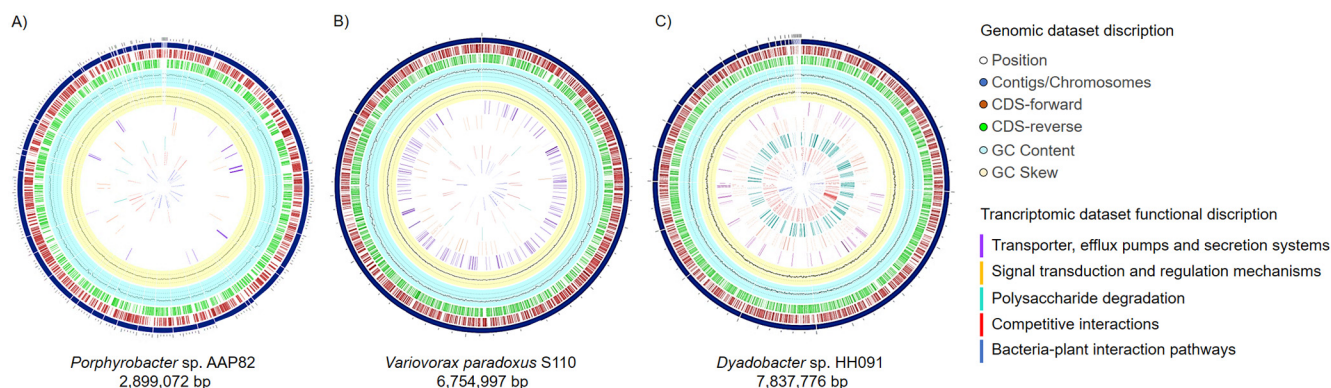
FIG 5 Metatranscriptome mapping to the reference genomes of *Porphyrobacter* sp. AAP82 (IMG 2551306481) (A), *Variovorax paradoxus* S110 (IMG 644736413) (B), and *Dyadobacter* sp. HH091 (IMG 222279) (C). Moving inward, the subsequent two rings show coding DNA sequences (CDSs) in forward (brown) and reverse (green) strands. Blue and yellow plots indicate GC content and a GC skew ([GC]/[G+C]]. Key features of possible competitive and plant-bacteria interaction pathways are marked with the following colors: purple, transporter, efflux pumps and secretion systems; orange, signal transduction and regulation mechanisms; green, polysaccharide degradation; red, competitive interactions; blue, bacteria-plant interaction pathways.

presented in all three bacteria, while biotin (B_7) pathway can be referred just to *Variovorax* (Fig. 4; Table S7).

Cell-cell communication as a key component of microbe-alga interaction. In the *Dyadobacter* genome the *darA* and *darB* genes, coding for the autoinducer synthase, were highly transcribed during exponential and stationary growth phases (6,376 and 12,094 hits). These genes are involved in the dialkylresorcinol synthesis gene cluster of *Dyadobacter*. Dialkylresorcinols are known as novel and widespread bacterial signaling molecules (23). Further analysis of the cell-cell communication as a key component of microbe-alga interaction identified two autoinducer synthase genes (i.e., *luxI* homologues) coding for *N*-acyl-L-homoserine lactone synthases in *Variovorax*.

Additional searches for QQ genes identified 19 genes that were mostly transcribed at the stationary growth phase. A potential dienelactone hydrolase from *Dyadobacter* revealed 1,110 counts and a *Porphyrobacter* homologue had 1,212 counts of mRNA reads.

Overall, among other components of cell signaling, we identified four *luxR* solo coding genes being highly expressed in *Dyadobacter* and having 4,429 counts. Similarly, in *Variovorax*, three *luxR* genes were found with 2,761 mRNA read counts during the stationary growth phase. A similar pattern was observed in the exponentially growing cultures (Fig. 4; Table S7).

Secretion systems are most relevant for competitive interaction. The analysis revealed secretion systems, which are known to be beneficial for bacterial surface colonization and for the algal-bacterial interactions (24, 25). T4SS, T6SS, and T9SS were expressed by the different bacteria. A more detailed inspection of the genomes revealed that *Dyadobacter* coded for T5SS, T6SS, and T9SS, whereas the genomes of *Porphyrobacter* and *Variovorax* coded for T2SS, T4SS, T5SS, and T6SS. Genes affiliated with T1SS and T3SS were not found during this analysis.

The T9SS was strongly expressed by *Dyadobacter*, with 12,967 hits in the exponential and 58,578 hits in the stationary growth phases. Other components of transport and secretion systems were upregulated during the stationary growth phase, often with gene hits that were twice as high. In our data set, *Variovorax* was the only bacterium that expressed the T2SS. While counting 1,843 hits during the exponential growth phase, this number gets doubled during the stationary phase. Gene counts for the T4SS found in *Porphyrobacter* during the exponential growth phase increased by a factor of 7 in the stationary phase.

***Dyadobacter* expresses many polysaccharide-modifying enzymes.** The Bacteroidetes phylum is known for its ability to degrade a wide range of polysaccharides, a trait that has enabled its dominance in many diverse environments, including plants and algal polysaccharides (26). As a member of this phylum, HH091, codes for a wealth of

polysaccharide-modifying enzymes, many of which were highly expressed (Table 1; Fig. 4). α-L-Fucosidases of GH29 and GH95 families were observed in the metatranscriptome. Highly transcribed genes also included a β-fructosidase, which belongs to the GH32 family. Additionally, genes predicted to be involved in chitin, xylan, xyloglucan, and galactoglucomannan utilization were highly expressed. Since HH091 was the most active organism to encode polysaccharide utilization loci (PULs), it revealed a remarkably high-level transcription of these genes. PULs of HH091 were expressed with 253,760 RNA-Seq reads at exponential and 486,271 at the stationary growth phase (Fig. 4).

Mutualism and commensalism as the main survival concepts in phycosphere. Fig. 4 reflects the expression of genes affiliated with competitive interaction of the microbiota. Genes that are responsible for competitive interaction pathways included potential antibiotic substance biosynthesis pathways, nucleases, permeases, proteases, and genes involved in heme biosynthesis. In addition, 128,759 hits were related to genes linked to reactive oxygen species (ROS) tolerance in the HH091 data set. During stationary growth phase, 89,165 hits versus 39,594 hits of exponential growth phase were observed (Fig. 4). The occurrence and expression of ROS tolerance genes in bacteria are essential for resistance to oxidative stress caused by the host (27).

The expression of invasion-associated proteins during the exponential growth phase is mostly negligible but gains importance during the stationary growth phase, as observed for *Variovorax* and *Dyadobacter* (Fig. 4). Further, we observed a relatively high number of hits for leucine-rich repeat (LRR) and invasion-associated proteins belonging to *Dyadobacter* and *Variovorax*. It is known that bacteria use LRR and invasion proteins as signaling and detecting components for the establishment of the interaction with the plant innate immune system (28).

Phytohormones biosynthesis systems essential for plant-bacteria liaison. Phytohormones play a vital role in plant growth and development as a regulator of numerous biological processes that can positively influence the growth and development of microalgae (8). To determine the involvement of the microalgae-growth-promoting substances, we have analyzed the enzymatic systems responsible for phytohormones biosynthesis. While *Dyadobacter* and *Porphyrobacter* appear to lack any genes affiliated with plant hormone production, the *Variovorax* genome codes for two enzymatic systems, nitrilase and nitrile hydratase/amidase, that are predicted to convert indole-3-acetonitrile to the plant hormone indole-3-acetic acid. *Variovorax* lacks tryptophan 2-monooxygenase, although it can produce indole-3-acetic acid using indole-3-acetonitrile as the precursor. In the transcriptome data, a total of 9,915 counts was linked to this pathway, implying that auxins are potentially produced and released. These data imply that *Variovorax* produces auxin-like molecules, possibly stimulating the growth of the microalga. Taken together, these data imply that each of the three bacteria transcribes a unique set of genes that are of relevance for synthesis of common goods and growth and survival of the whole community.

DISCUSSION

A comprehensive understanding of the composition of the microbial community, as well as competitive interaction, is required to create scientific and theoretical fundamentals of interaction mechanisms between microalgae and other microorganisms, including the development of effective processes for simultaneous algal cultivation with enhancing the efficiency of microalgae biomass growth and associated valuable compounds production.

Specialized distribution of assignments at algae-bacterial phycosphere. The evaluation of the top 250 gene hits resulted in the identification of genes related to the general metabolic activities, carbohydrate degradation, biofilm formation, transport mechanisms, and secretion systems, which support the distribution of assignments at the microbial consortium. Former reports on the relationships within the microalga-bacteria consortia have also provided a blueprint for the construction of mutually beneficial synthetic ecosystems, in which the general metabolic activities played a significant role (29–31).

Many pathogenic bacteria are known to use secretion systems for the facilitation of their proliferation and survival inside eukaryotic hosts, typically by the secretion of protein effectors or protein-DNA complexes (32). The presence of T6SS suggests the distribution of tasks among members of studied consortia, providing the fitness and colonization advantages, which are not restricted to virulence. T9SS machinery components, established for *Dyadobacter* within the Bacteroidota phylum, represents the assembly of the gliding motility apparatus and possible external release of proteins with various functions, including cell surface exposition, attachment, and other virulence factors (33, 34). The widespread occurrence of gliding motility genes was previously revealed among the members of the same phylum, the gliding bacterium *Flavobacterium johnsoniae*, and the nonmotile oral pathogen *Porphyromonas gingivalis*. *F. johnsoniae* uses T9SS as the gliding motility apparatus and for the secretion of a chitinase that is required for chitin digestion, and the *P. gingivalis* secretes through this system gingipain protease virulence factors. The same route likely secretes other polysaccharide-digesting enzymes produced by other members of the phylum. The mechanisms underlying the processes of gliding motility and cell surface machinery to utilize polysaccharides remain unclear (35, 36). Nevertheless, it is known that T9SS machinery secretes most of CAZymes, such as GHs, PLs, CEs, and accessory proteins (37, 38).

Complex relationships through competition and synergy in algae-bacterial phycosphere biofilms. Studying the interactions between members of alga-bacterial phycosphere, we investigated the hypothesis that dominant bacterial members possess the role of superior competitors. Members of the microbiome of *S. quadricauda* participate in the consortium niche in a competitive way that is reflected in a heat map with the correspondence to genes, affiliated with potential antibiotic substances, endonucleases and exonucleases, permeases, proteases, heme synthesis, and QQ (Fig. 4), which are known as important factors required for biofilm formation, virulence, and competition (39–42). The analysis of the microbiome of *S. Quadricauda* revealed different proteins supposed to be beneficial during competition for space and nutrients on surfaces in biofilms. Bacterial dominance can be attributed to the ability of these organisms to rapidly form microcolonies and their ability to produce extracellular antibacterial compounds (43). The *S. quadricauda* microbiome is composed of single-species populations or mixed populations with various levels of interaction, depending on the exponential or stationary growth phase. *Porphyrobacter*, *Dyadobacter*, and *Variovorax* were found to be the dominant producers of numerous antibacterial proteins, which can possibly eliminate other microorganisms or exhibit strong inhibitory activity against them.

The signaling molecules related to QS and QQ activity were affiliated with the Alphaproteobacteriota and Bacteroidota. Among metatranscriptome data sets proteins predicted as QQ included dienelactone hydrolase, imidazolonepropionase, 6-phosphogluconolactonase, gluconolactonase, oxidoreductases, and metal-dependent hydrolases of the β-lactamase superfamily, related to QQ activity. Highly transcribed genes were observed, mostly at the stationary growth phase, that fulfill the competitive needs of bacteria to comprise one of the dominant heterotrophic bacterial groups in aquaculture, which are represented in Fig. 4. Dienelactone hydrolase, known as a QQ enzyme that degrades or modifies *N-Acyl* homoserine lactones (AHLs) (44, 45), was established for *Dyadobacter* and *Porphyrobacter*. Gluconolactonases, reported as quorum-quenching enzymes (46), were mapped to *Dyadobacter*. Another class of enzyme, oxidoreductase, established to catalyze the oxidation or reduction of acyl side chain (33, 34), originated in *Variovorax* and *Dyadobacter*. The analysis also revealed several phenotypes beneficial for bacterial surface colonization, including motility, exopolysaccharide production, biofilm formation, and toxin production (Fig. 4), which are often regulated by QS (8, 16, 17).

Simultaneously, several members of the *S. quadricauda* microbiome appeared to be the main suppliers of vitamins to microalga. Genes involved in thiamin, cobalamin, biotin, and riboflavin synthesis were established for Alphaproteobacteriota and Cytophagaceae, which confirms the strong evidence that alga-associated bacteria are responsible for the supply of the essential vitamins to alga (19). Thus, our study shows that this interaction involves the strong collaboration between members of the alga-bacterial phycosphere

with the support of nutritive components and the synergetic exchange of biosynthetic compounds.

A significant number of genes of high importance for root colonization, biofilm formation, invasion (47, 48), virulence, and pathogenicity were identified (49–51). Fig. 4 describes genes affiliated with overall plant-bacteria interaction pathways, including ROS tolerance, LRR proteins, and invasion-associated proteins. Numerous genes responsible for the ROS tolerance were highly transcribed at the stationary phase, which explains the necessity of bacteria to protect itself from massive amounts of reactive oxygen species released by microalgae, which was previously suggested to expose them to pathogens (28). It is supposed that dominating microorganisms can use LRR and invasion proteins as a signaling and detecting components for the establishment of the interaction with the possible innate immune system of the *S. quadricauda*.

In summary, the current study gives a detailed insight into mutualistic collaboration of microalgae and bacteria, including the involvement of competitive interplay between bacteria. Future work will now have to unravel the signaling between the bacteria and eukaryotes, as well as the detailed nutrient exchange and mutual support in different aspects of cross-kingdom synergistic network.

MATERIALS AND METHODS

Microorganisms used in this study and cultivation media. *S. quadricauda* MZCH 10104 was obtained from the Microalgae and Zygnematophyceae Collection Hamburg (MZCH) and cultivated in BG11 medium at 20 ± 1°C and 100 ± 10 μmol photons m^{-2} s^{-1} with a 14-h light/10-h dark schedule (19, 52, 53). To maintain the axenity of the algal culture, *S. quadricauda* was treated with the antibiotic cocktail: penicillin G, streptomycin sulfate, and gentamicin sulfate (100, 25, and 25 mg/L, respectively) (54–56).

The media for cultivation of individual bacterial isolates derived from the microalgae-associated community were prepared as follows. R2A medium and TYES were prepared as described previously (57, 58), and M9, TSB, and NB media were prepared according to the method of Sambrook and Russell (59). To stimulate microbial growth, the media were in part supplemented with algal culture extracts during the exponential and stationary growth phase of the microalgae ranging from 5 to 50% (vol/vol). The inoculated plates were incubated for 5 to 7 days at 22°C under aerobic and anaerobic conditions.

Dyadobacter sp. HH091 was isolated during this work from a laboratory culture of *S. quadricauda* MZCH 10104. The isolate was routinely grown in 5 mL of tryptone yeast extract salts (TYES) broth at 22°C for 3 to 4 days at 200 rpm (60).

Coculturing procedure and conditions. *S. quadricauda* MZCH 10104 and *Dyadobacter* sp. HH091 were cocultured in BG11 medium at 20 ± 1°C and 100 ± 10 μmol photons m^{-2} s^{-1} with a 14-h light/10-h dark schedule over a time period of 13 days. Therefore, 1 mL of *S. quadricauda* was treated with an antibiotic cocktail of penicillin$_{100}$, streptomycin$_{25}$, and gentamycin$_{25}$ in 50 mL of BG11 medium to remove all bacteria. The antibiotic treatment was performed for 1 day. Afterwards, the microalga was centrifuged (5,000 rpm for 10 min) and washed two times with 1 mL BG11 and finally resuspended in 50 mL of BG11 medium, where it was grown for 13 days. At the start of the experiment, each flask contained 50 mL of BG11, *S. quadricauda* (optical density at 750 nm [OD$_{750nm}$] = 0.03), and *Dyadobacter* (OD$_{600nm}$ = 0.05).

Bacterial RNA extraction and sequencing. The hot phenol method with minor modifications was used to extract the total RNA (19, 61). RNA quality was checked using a 2100 Bioanalyzer with the RNA 6000 Nano kit (Agilent Technologies). The RNA integrity number (RIN) for all samples was ≥ 7. Equal amounts of the remaining transcripts and kit components were used for cDNA library construction. Libraries suitable for sequencing were prepared from 400 and 275 ng of total RNA with oligo(dT) capture beads for poly(A) mRNA enrichment using the TruSeq stranded mRNA library preparation kit (Illumina) according to the manufacturer's instructions. After 14 cycles of PCR amplification, the size distribution of the barcoded DNA libraries was estimated $\sim$300 bp by electrophoresis on Agilent DNA HS bioanalyzer microfluidic chips.

Sequencing of pooled libraries spiked with 5% PhiX control library was performed at 8 million reads/sample in paired-end mode with 150-nucleotide (nt) read length on the NextSeq 500 platform (Illumina) using a High Output 400M sequencing kit. Demultiplexed FASTQ files were generated with bcl2fastq2 v2.20.0.422 (Illumina).

Processing and analysis of RNA-Seq reads. Fastp (v0.21.0) was used to remove artificial and low-quality (Phred quality score below 15) sequences from the 3′-end of sequence reads (62). Putative base calling errors located in regions were two reads of a read pair overlap were corrected (option: –correction). Kraken2 (v2.1.2) was used in combination with Bracken (v2.6.2) to assess the taxonomic composition (63, 64). Additionally, reads were assembled with Trinity (v2.13.2) (65). Assembly statistics were assessed with Quast (v5.0.2) (66). The resulting contigs were aligned to sequences present in the UniProtKB/Swiss-Prot database (release 2021_04) and taxonomically annotated accordingly (67). Both were achieved with Mmseqs2 (version ad5837b3444728411e6c90f8c6ba9370f665c443) in "easy taxonomy" mode (–lca-mode 4) (68).

Total bacterial DNA extraction. Genomic DNA of pure cultures of the strain *Dyadobacter* sp. HH091 was extracted using the peqGOLD bacterial DNA kit (PEQLAB Biotechnologie GmbH, Erlangen, Germany) according to the manufacturer's instructions.

***Dyadobacter* sp. HH091 transformation.** The strain HH091 was transformed with modified plasmid pBBR1MCS-5-eGFP by electroporation according to standard methods, which resulted in bright green fluorescent colonies as observed by fluorescence microscopy (59). The plasmid contains the broad-host-range vector pBBR1MCS-5, providing a gentamicin resistance and the expression of GFP. Gentamycin was provided at 100 μg/mL, and the bacteria were grown for 3 to 4 days at 22°C in liquid medium or on a plate.

Bacterial genome sequencing, *de novo* assembly, and binning. Total genomic DNA of *Dyadobacter* sp. HH091 was extracted for a genomic analysis using the NucleoBond high-molecular-weight genomic DNA kit for microorganisms (Macherey-Nagel, Germany) following the manufacturer's instructions and a previously published enzymatic cell lysis protocol with some modifications, including freezing in liquid nitrogen, bead beating, and an additional lysis pretreatment with proteinase K and lysozyme for 24 h at 55°C (2). The extracted DNA was sequenced on an Illumina NextSeq 500 platform using rapid sequencing by synthesis (SBS) chemistry v2 (Illumina, San Diego). For this, the DNA library was constructed applying the NEBNext Ultra II DNA library prep kit for Illumina (New England Biolabs) according to the manufacturer's protocol. Initial fragmentation of DNA was performed on the Bioruptor NGS (Diagenode) with 30 s on/30 s off for 16 cycles. Sequencing of the metagenomic DNA library was performed on the NextSeq 500 platform (Illumina) as paired-end run (2 × 150 cycles) with ~60 mio reads. Fastp (v0.21.0) was used to remove artificial and low-quality (Phred quality score below 15) sequences from the 3'-end of sequence reads. Putative base calling errors located in regions were two reads of a read pair overlap were corrected (Fastp option: –correction). Reads shorter than 40 bp were discarded. Sequence reads were than assembled using SPAdes (v3.15.3) (69). The final draft assembly consists of 7,862,706 bp with a GC content of 43.81%. The final genome assembly resulted in 2,018 contigs (N50, 607,803 bp; L50, 10), with a largest contig size of 1,195,963 bp.

Physiological analyses. (i) Microscopy investigations. *Dyadobacter* sp. HH091 expressing eGFP was cocultured with *S. quadricauda* MZCH 10104 and studied using a confocal laser scanning microscope (CLSM) Axio Observer.Z1/7 LSM 800 (Carl Zeiss Microscopy GmbH, Jena, Germany), including Z-Stack microscope techniques. The analysis of the CLSM images were done with ZEN software (version 2.3; Carl Zeiss Microscopy GmbH). An improved 4'-6-diamidino-2-phenylindole (DAPI) staining procedure with some modifications was used in microscopy investigations (70). Modifications included the treatment with the TrueVIEW autofluorescence quenching kit (Vector Labs, SP-8400), which was employed to enhance staining and to lower the autofluorescence of chlorophyll of the microalga known to be troublesome. Background autofluorescence occurring in the 600- to 700-nm range makes it impossible to detect the bacteria transformed with plasmids expressing fluorescent proteins. The TrueVIEW Quencher is an aqueous solution of a hydrophilic molecule, which binds to chlorophyll electrostatically and lowers the fluorescence (71).

(ii) Pulse-amplitude-modulation (PAM) fluorometry. The photosynthetic activity of microalgae was measured by pulse-amplitude-modulation (PAM) fluorometry. The measured parameters represent the optimal quantum yield of PS II photochemistry (F_v/F_m), with the fluorescence (F_0) measured during the illumination of a pre-dark-adapted sample with open reaction centers and under saturating light with closed reaction centers is the maximum fluorescence (F_m). The difference $F_m - F_0$, is called variable fluorescence (F_v), representing the amount of light energy that can be used by PS II (72).

(iii) Fluorescence-activated cell sorting (FACS). Flow cytometry was applied to analyze the chlorophyll content of *S. quadricauda* cocultivated with *Dyadobacter* sp. HH091. An antibiotic-treated algae culture without *Dyadobacter* sp. served as a control. Growth of *S. quadricauda* was monitored over 13 days after inoculation (start OD_{750nm} = 0.090) with and without *Dyadobacter* sp. (OD_{600nm} = 0.05). Culture samples with volumes of 1 mL (with and without *Dyadobacter*) were withdrawn in triplicate for the experiments every 3 days. For every measurement, we used 0.5 mL of algal culture diluted in 0.5 mL of BG11 medium and filtered through a 35-μm Strainer cap. The samples were subjected to flow cytometry using the S3e cell sorter (Bio-Rad, Hercules, CA) equipped with a 488-nm excitation laser and detectors for side and forward scatter (i.e., SSC and FSC area), FL1 (525/30-nm band pass filter), and FL2 (560-nm long-pass filter). Data analysis was carried out with the FlowJo software package (v10.6.1; BD Life Science, Ashlan, OR). The FL2 detector allowed detection of the chlorophyll autofluorescence of *S. quadricauda*, and the culture samples were analyzed in a two-dimensional density plot of FL2 area versus FSC area to identify algal cells with elevated and reduced chlorophyll levels, and bacteria to determine the relative ratio of each population. The identity (algae or bacteria) and physiological state (live or dead algae) of the populations, detected in the FL2-FCS area plot, was confirmed by microscopy after sorting the respective subpopulations with the cell sorting function (purity mode) of the cell sorter instrument. For each sample the measurement was normalized until 15,000 events.

Data availability. Sequences obtained for this study were submitted to the European Nucleotide Archive (ENA). They are publicly available under accession number PRJEB23338. Assembly of the *Dyadobacter* sp. HH091 genome is available via IMG/M (https://img.jgi.doe.gov) using IMG ID 2842103827.

SUPPLEMENTAL MATERIAL

Supplemental material is available online only.

SUPPLEMENTAL FILE 1, PDF file, 2.7 MB.

REFERENCES

1. Fulbright SP, Robbins-Pianka A, Berg-Lyons D, Knight R, Reardon KF, Chisholm ST. 2018. Bacterial community changes in an industrial algae production system. Algal Res 31:147–156. https://doi.org/10.1016/j.algal.2017.09.010.
2. Krohn-Molt I, Wemheuer B, Alawi M, Poehlein A, Güllert S, Schmeisser C, Pommerening-Röser A, Grundhoff A, Daniel R, Hanelt D, Streit WR. 2013. Metagenome survey of a multispecies and alga-associated biofilm revealed key elements of bacterial-algal interactions in photobioreactors. Appl Environ Microbiol 79:6196–6206. https://doi.org/10.1128/AEM.01641-13.
3. Cirri E, Pohnert G. 2019. Algae-bacteria interactions that balance the planktonic microbiome. New Phytol 223:100–106. https://doi.org/10.1111/nph.15765.
4. Ramanan R, Kim BH, Cho DH, Oh HM, Kim HS. 2016. Algae-bacteria interactions: evolution, ecology and emerging applications. Biotechnol Adv 34:14–29. https://doi.org/10.1016/j.biotechadv.2015.12.003.
5. Fuentes JL, Garbayo I, Cuaresma M, Montero Z, González-Del-Valle M, Vílchez C. 2016. Impact of microalgae-bacteria interactions on the production of algal biomass and associated compounds. Mar Drugs 14:100. https://doi.org/10.3390/md14050100.
6. Lee JK, Park KS, Park MS, Kim SM, Chung SY, Lee DS. 2013. Surgical treatment of lumbar hyperextension injury in ankylosing spondylitis. Korean J Spine 10:195–199. https://doi.org/10.14245/kjs.2013.10.3.195.
7. Whitman T, Neurath R, Perera A, Chu-Jacoby I, Ning D, Zhou J, Nico P, Pett-Ridge J, Firestone M. 2018. Microbial community assembly differs across minerals in a rhizosphere microcosm. Environ Microbiol 20:4444–4460. https://doi.org/10.1111/1462-2920.14366.
8. Davies DG, Parsek MR, Pearson JP, Iglewski BH, Costerton JW, Greenberg EP. 1998. The involvement of cell-to-cell signals in the development of a bacterial biofilm. Science 280:295–298. https://doi.org/10.1126/science.280.5361.295.
9. Segev E, Wyche TP, Kim KH, Petersen J, Ellebrandt C, Vlamakis H, Barteneva N, Paulson JN, Chai L, Clardy J, Kolter R. 2016. Dynamic metabolic exchange governs a marine algal-bacterial interaction. Elife 5:e17473. https://doi.org/10.7554/eLife.17473.
10. Wang H, Tomasch J, Jarek M, Wagner-Döbler I. 2014. A dual-species co-cultivation system to study the interactions between Roseobacters and dinoflagellates. Front Microbiol 5:311. https://doi.org/10.3389/fmicb.2014.00311.
11. Mouget J, Dakhama A, Lavoie MC, Noüe JD. 1995. Algal growth enhancement by bacteria: is consumption of photosynthetic oxygen involved? FEMS Microbiol Ecol 18:35–43. https://doi.org/10.1016/0168-6496(95)00038-C.
12. Wieczorek AS, Schmidt O, Chatzinotas A, von Bergen M, Gorissen A, Kolb S. 2019. Ecological functions of agricultural soil bacteria and microeukaryotes in chitin degradation: a case study. Front Microbiol 10:1293. https://doi.org/10.3389/fmicb.2019.01293.
13. Shen Y, Benner R. 2018. Mixing it up in the ocean carbon cycle and the removal of refractory dissolved organic carbon. Sci Rep 8:2542. https://doi.org/10.1038/s41598-018-20857-5.
14. Käse L, Geuer JK. 2018. Phytoplankton responses to marine climate change – an introduction, p 55–71. In Jungblut S, Liebich V, Bode M (eds), YOUMARES 8 – oceans across boundaries: learning from each other. Springer, Cham, Switzerland.
15. Luo H, Moran MA, Luo H, Moran MA. 2014. Evolutionary ecology of the marine Roseobacter clade. Microbiol Mol Biol Rev 78:573–587. https://doi.org/10.1128/MMBR.00020-14.
16. Stoodley P, Sauer K, Davies DG, Costerton JW. 2002. Biofilms as complex differentiated communities. Annu Rev Microbiol 56:187–209. https://doi.org/10.1146/annurev.micro.56.012302.160705.
17. Parsek MR, Greenberg EP. 2005. Sociomicrobiology: the connections between quorum sensing and biofilms. Trends Microbiol 13:27–33. https://doi.org/10.1016/j.tim.2004.11.007.
18. Phour M, Sehrawat A, Sindhu SS, Glick BR. 2020. Interkingdom signaling in plant-rhizomicrobiome interactions for sustainable agriculture. Microbiol Res 241:126589. https://doi.org/10.1016/j.micres.2020.126589.
19. Krohn-Molt I, Alawi M, Förstner KU, Wiegandt A, Burkhardt L, Indenbirken D, Thieß M, Grundhoff A, Kehr J, Tholey A, Streit WR. 2017. Insights into microalga and bacteria interactions of selected phycosphere biofilms using metagenomic, transcriptomic, and proteomic approaches. Front Microbiol 8:1941. https://doi.org/10.3389/fmicb.2017.01941.
20. Li X, Koblížek M, Feng F, Li Y, Jian J, Zeng Y. 2013. Whole-genome sequence of a freshwater aerobic anoxygenic phototroph, Porphyrobacter sp. Strain AAP82, isolated from the Huguangyan Maar Lake in Southern China. Genome Announc 1:e0007213. https://doi.org/10.1128/genomeA.00072-13.
21. Han J-I, Choi H-K, Lee S-W, Orwin PM, Kim J, Laroe SL, Kim T-G, O'Neil J, Leadbetter JR, Lee SY, Hur C-G, Spain JC, Ovchinnikova G, Goodwin L, Han C. 2011. Complete genome sequence of the metabolically versatile plant growth-promoting endophyte Variovorax paradoxus S110. J Bacteriol 193:1183–1190. https://doi.org/10.1128/JB.00925-10.
22. Moore SJ, Warren MJ. 2012. The anaerobic biosynthesis of vitamin B$_{12}$. Biochem Soc Trans 40:581–586. https://doi.org/10.1042/BST20120066.
23. Brameyer S, Kresovic D, Bode HB, Heermann R. 2015. Dialkylresorcinols as bacterial signaling molecules. Proc Natl Acad Sci U S A 112:572–577. https://doi.org/10.1073/pnas.1417685112.
24. Lucke M, Correa MG, Levy A. 2020. The role of secretion systems, effectors, and secondary metabolites of beneficial rhizobacteria in interactions

with plants and microbes. Front Plant Sci 11:589416. https://doi.org/10.3389/fpls.2020.589416.

25. Zboralski A, Biessy A, Filion M. 2022. Bridging the gap: type III secretion systems in plant-beneficial bacteria. Microorganisms 10:187. https://doi.org/10.3390/microorganisms10010187.

26. McKee LS, La Rosa SL, Westereng B, Eijsink VG, Pope PB, Larsbrink J. 2021. Polysaccharide degradation by the Bacteroidetes: mechanisms and nomenclature. Environ Microbiol Rep 13:559–581. https://doi.org/10.1111/1758-2229.12980.

27. Fones H, Preston GM. 2012. Reactive oxygen and oxidative stress tolerance in plant pathogenic Pseudomonas. FEMS Microbiol Lett 327:1–8. https://doi.org/10.1111/j.1574-6968.2011.02449.x.

28. Im SH, Klochkova TA, Lee DJ, Gachon CMM, Kim GH. 2019. Genetic toolkits of the red alga Pyropia tenera against the three most common diseases in Pyropia farms. J Phycol 55:801–815. https://doi.org/10.1111/jpy.12857.

29. Blifernez-Klassen O, Klassen V, Wibberg D, Cebeci E, Henke C, Rückert C, Chaudhari S, Rupp O, Blom J, Winkler A, Al-Dilaimi A, Goesmann A, Sczyrba A, Kalinowski J, Bräutigam A, Kruse O. 2021. Phytoplankton consortia as a blueprint for mutually beneficial eukaryote-bacteria ecosystems based on the biocoenosis of Botryococcus consortia. Sci Rep 11:1726. https://doi.org/10.1038/s41598-021-81082-1.

30. Seymour JR, Amin SA, Raina J-B, Stocker R. 2017. Zooming in on the phycosphere: the ecological interface for phytoplankton–bacteria relationships. Nat Microbiol 2:17065. https://doi.org/10.1038/nmicrobiol.2017.65.

31. Amin SA, Parker MS, Armbrust EV. 2012. Interactions between diatoms and bacteria. Microbiol Mol Biol Rev 76:667–684. https://doi.org/10.1128/MMBR.00007-12.

32. Gonzalez-Rivera C, Bhatty M, Christie PJ. 2016. Mechanism and function of type IV secretion during infection of the human host. Microbiol Spectr 4:https://doi.org/10.1128/microbiolspec.VMBF-0024-2015. https://doi.org/10.1128/microbiolspec.VMBF-0024-2015.

33. Uroz S, Chhabra SR, Cámara M, Williams P, Oger P, Dessaux Y. 2005. N-Acylhomoserine lactone quorum-sensing molecules are modified and degraded by Rhodococcus erythropolis W2 by both amidolytic and novel oxidoreductase activities. Microbiology 151:3313–3322. https://doi.org/10.1099/mic.0.27961-0.

34. Chowdhury PK, Keshavan N, Nguyen HQ, Peterson JA, González JE, Haines DC. 2007. Bacillus megaterium CYP102A1 oxidation of acyl homoserine lactones and acyl homoserines. Biochemistry 46:14429–14437. https://doi.org/10.1021/bi701945j.

35. McBride MJ, Zhu Y. 2013. Gliding motility and Por secretion system genes are widespread among members of the phylum Bacteroidetes. J Bacteriol 195:270–278. https://doi.org/10.1128/JB.01962-12.

36. Saiki K, Konishi K. 2007. Identification of a Porphyromonas gingivalis novel protein Sov required for the secretion of gingipains. Microbiol Immunol 51:483–491. https://doi.org/10.1111/j.1348-0421.2007.tb03936.x.

37. Cantarel BL, Coutinho PM, Rancurel C, Bernard T, Lombard V, Henrissat B. 2009. The Carbohydrate-Active EnZymes Database (CAZy): an expert resource for glycogenomics. Nucleic Acids Res 37:D233–D238. https://doi.org/10.1093/nar/gkn663.

38. Henrissat B. 1991. A classification of glycosyl hydrolases based on amino acid sequence similarities. The Biochemical J 280:309–316. https://doi.org/10.1042/bj2800309.

39. Nocek B, Tikhonov A, Babnigg G, Gu M, Zhou M, Makarova KS, Vondenhoff G, Van Aerschot A, Kwon K, Anderson WF, Severinov K, Joachimiak A. 2012. Structural and functional characterization of microcin C resistance peptidase MccF from Bacillus anthracis. J Mol Biol 420:366–383. https://doi.org/10.1016/j.jmb.2012.04.011.

40. Gristwood T, McNeil MB, Clulow JS, Salmond GPC, Fineran PC. 2011. PigS and PigP regulate prodigiosin biosynthesis in serratia via differential control of divergent operons, which include predicted transporters of sulfur-containing molecules. J Bacteriol 193:1076–1085. https://doi.org/10.1128/JB.00352-10.

41. Ge X, Kitten T, Chen Z, Lee SP, Munro CL, Xu P. 2008. Identification of Streptococcus sanguinis genes required for biofilm formation and examination of their role in endocarditis virulence. Infect Immun 76:2551–2559. https://doi.org/10.1128/IAI.00338-08.

42. Choby JE, Skaar EP. 2016. Heme synthesis and acquisition in bacterial pathogens. J Mol Biol 428:3408–3428. https://doi.org/10.1016/j.jmb.2016.03.018.

43. Rao D, Webb JS, Kjelleberg S. 2005. Competitive interactions in mixed-species biofilms containing the marine bacterium Pseudoalteromonas tunicata. Appl Environ Microbiol 71:1729–1736. https://doi.org/10.1128/AEM.71.4.1729-1736.2005.

44. Schipper C, Hornung C, Bijtenhoorn P, Quitschau M, Grond S, Streit WR. 2009. Metagenome-derived clones encoding two novel lactonase family proteins involved in biofilm inhibition in Pseudomonas aeruginosa. Appl Environ Microbiol 75:224–233. https://doi.org/10.1128/AEM.01389-08.

45. Krysciak D, Schmeisser C, Preuss S, Riethausen J, Quitschau M, Grond S, Streit WR. 2011. Involvement of multiple loci in quorum quenching of autoinducer I molecules in the nitrogen-fixing symbiont Rhizobium (Sinorhizobium) sp. Strain NGR234. Appl Environ Microbiol 77:5089–5099. https://doi.org/10.1128/AEM.00112-11.

46. Ogawa K, Nakajima-Kambe T, Nakahara T, Kokufuta E. 2002. Coimmobilization of gluconolactonase with glucose oxidase for improvement in kinetic property of enzymatically induced volume collapse in ionic gels. Biomacromolecules 3:625–631. https://doi.org/10.1021/bm025512f.

47. Desvaux M, Hébraud M. 2006. The protein secretion systems in Listeria: inside out bacterial virulence. FEMS Microbiol Rev 30:774–805. https://doi.org/10.1111/j.1574-6976.2006.00035.x.

48. Pilgrim S, Kolb-Mäurer A, Gentschev I, Goebel W, Kuhn M. 2003. Deletion of the gene encoding p60 in Listeria monocytogenes leads to abnormal cell division and loss of actin-based motility. Infect Immun 71:3473–3484. https://doi.org/10.1128/IAI.71.6.3473-3484.2003.

49. Breidenstein EB, Janot L, Strehmel J, Fernandez L, Taylor PK, Kukavica-Ibrulj I, Gellatly SL, Levesque RC, Overhage J, Hancock RE. 2012. The Lon protease is essential for full virulence in Pseudomonas aeruginosa. PloS One 7:e49123. https://doi.org/10.1371/journal.pone.0049123.

50. Cuthbertson L, Mainprize IL, Naismith JH, Whitfield C. 2009. Pivotal roles of the outer membrane polysaccharide export and polysaccharide copolymerase protein families in export of extracellular polysaccharides in Gram-negative bacteria. Microbiol Mol Biol Rev 73:155–177. https://doi.org/10.1128/MMBR.00024-08.

51. Zografou C, Dimou M, Katinakis P. 2020. FK506-binding protein FklB is involved in biofilm formation through its peptidyl-prolyl isomerase activity. bioRxiv. https://doi.org/10.1101/2020.02.01.930347.

52. Stanier RY, Kunisawa R, Mandel M, Cohen-Bazire G. 1971. Purification and properties of unicellular blue-green algae (order Chroococcales). Bacteriol Rev 35:171–205. https://doi.org/10.1128/br.35.2.171-205.1971.

53. Rippka R, Deruelles J, Waterbury JB, Herdman M, Stanier RY. 1979. Generic assignments, strain histories and properties of pure cultures of Cyanobacteria. Microbiology 111:1–61. https://doi.org/10.1099/00221287-111-1-1.

54. Lee HG, Shin SY, Jin L, Yoo C, Srivastava A, La HJ, Ahn CY, Kim HS, Oh HM. 2015. Establishment and maintenance of an axenic culture of Ettlia sp. Using a species-specific approach. Biotechnol Bioproc E 20:1056–1063. https://doi.org/10.1007/s12257-015-0289-4.

55. Droop MR. 1967. A procedure for routine purification of algal cultures with antibiotics. British Phycological Bull 3:295–297. https://doi.org/10.1080/00071616700650171.

56. Andersen RA. 2005. Algal culturing techniques. Phycological Society of America, College Park, MD.

57. Reasoner DJ, Geldreich EE. 1985. A new medium for the enumeration and subculture of bacteria from potable water. Appl Environ Microbiol 49:1–7. https://doi.org/10.1128/aem.49.1.1-7.1985.

58. Holt RA. 1993. Bacterial cold-water disease, p 3–22. In Inglis V, Roberts RJ, Bromage NR (ed), Bacterial diseases of fish. Wiley-Blackwell, Hoboken, NJ.

59. Sambrook JF, Russell D. 2001. Molecular cloning: a laboratory manual, vol. 1. Cold Spring Harbor Laboratory Press, Cold Spring Harbor, NY.

60. Holt RA. 1987. Cytophaga psychrophila, the causative agent of bacterial cold-water disease in salmonid fish. Philosophy 855:115.

61. Aiba H, Adhya S, de Crombrugghe B. 1981. Evidence for two functional gal promoters in intact Escherichia coli cells. J Biol Chem 256:11905–11910. https://doi.org/10.1016/S0021-9258(19)68491-7.

62. Chen S, Zhou Y, Chen Y, Gu J. 2018. Fastp: an ultra-fast all-in-one FASTQ preprocessor. Bioinformatics 34:i884–i890. https://doi.org/10.1093/bioinformatics/bty560.

63. Wood DE, Salzberg SL. 2014. Kraken: ultrafast metagenomic sequence classification using exact alignments. Genome Biol 15:R46. https://doi.org/10.1186/gb-2014-15-3-r46.

64. Lu J, Breitwieser FP, Thielen P, Salzberg SL. 2017. Bracken: estimating species abundance in metagenomics data. PeerJ Computer Science 3:e104. https://doi.org/10.7717/peerj-cs.104.

65. Grabherr MG, Haas BJ, Yassour M, Levin JZ, Thompson DA, Amit I, Adiconis X, Fan L, Raychowdhury R, Zeng Q, Chen Z, Mauceli E, Hacohen N, Gnirke A, Rhind N, di Palma F, Birren BW, Nusbaum C, Lindblad-Toh K, Friedman N, Regev A. 2011. Full-length transcriptome assembly from RNA-Seq data without a reference genome. Nat Biotechnol 29:644–652. https://doi.org/10.1038/nbt.1883.

66. Gurevich A, Saveliev V, Vyahhi N, Tesler G. 2013. QUAST: quality assessment tool for genome assemblies. Bioinformatics 29:1072–1075. https://doi.org/10.1093/bioinformatics/btt086.

67. UniProt Consortium. 2021. UniProt: the universal protein knowledgebase in 2021. Nucleic Acids Res 49:D480–D489. https://doi.org/10.1093/nar/gkaa1100.

68. Steinegger M, Söding J. 2017. Mmseqs2 enables sensitive protein sequence searching for the analysis of massive data sets. Nat Biotechnol 35:1026–1028. https://doi.org/10.1038/nbt.3988.

69. Bankevich A, Nurk S, Antipov D, Gurevich AA, Dvorkin M, Kulikov AS, Lesin VM, Nikolenko SI, Pham S, Prjibelski AD, Pyshkin AV, Sirotkin AV, Vyahhi N, Tesler G, Alekseyev MA, Pevzner PA. 2012. SPAdes: a new genome assembly algorithm and its applications to single-cell sequencing. J Comput Biol 19:455–477. https://doi.org/10.1089/cmb.2012.0021.

70. Mukherjee C, Mukherjee C, Ray K. 2015. An improved DAPI staining procedure for visualization of polyphosphate granules in cyanobacterial and microlagal cells. Protocol Exchange https://doi.org/10.1038/protex.2015.066.

71. Karpishin T. 2018. Reducing tissue autofluorescence. Genetic Engineering & Biotechnology News 38:16–17. https://doi.org/10.1089/gen.38.05.05.

72. Maxwell K., Johnson G., Maxwell K., Johnson GN. 2000. Chlorophyll fluorescence — a practical guide. J Exp Bot 51:659–668. https://doi.org/10.1093/jexbot/51.345.659.